
Multi-Objective Reinforcement Learning for Infectious Disease Control with Application to COVID-19 Spread

Runzhe Wan, Xinyu Zhang, Rui Song

Department of Statistics, North Carolina State University
 rwan@ncsu.edu, xzhang97@ncsu.edu, rsong@ncsu.edu

Abstract

Severe infectious diseases such as the novel coronavirus (COVID-19) pose a huge threat to public health. Stringent control measures, such as school closures and stay-at-home orders, while having significant effects, also bring huge economic losses. A crucial question for policymakers around the world is how to make the trade-off and implement the appropriate interventions. In this work, we propose a Multi-Objective Reinforcement Learning framework to facilitate the data-driven decision making and minimize the long-term overall cost. Specifically, at each decision point, a Bayesian epidemiological model is first learned as the environment model, and then we use the proposed model-based multi-objective planning algorithm to find a set of Pareto-optimal policies. This framework, combined with the prediction bands for each policy, provides a real-time decision support tool for policymakers. The application is demonstrated with the spread of COVID-19 in China.

1 Introduction

The novel coronavirus (COVID-19) has spread rapidly and posed a tremendous threat to the global public health (Organization et al. 2020). Among the efforts to contain its spread, several strict control measures, including school closures and workplace shutdowns, have shown high effectiveness (Anderson et al. 2020). Nevertheless, these measures always bring enormous costs to economies and other public welfare aspects (Eichenbaum, Rebelo, and Trabandt 2020). For example, an unprecedented unemployment rate in the United States partially caused by some COVID-19 control measures is anticipated by economists (Gangopadhyaya and Garrett 2020). In the face of an emerging infectious disease, we usually have multiple objectives conflicting with each other, and either overreaction or under-reaction may result in a substantial unnecessary loss. A crucial question for policymakers around the world is how to make the trade-off and intervene at the right time and in the right amount to minimize the overall long-term cost to the citizens.

Contribution. This paper aims to provide a real-time data-driven decision support tool for policymakers. We formalize the problem under the multi-objective Markov decision process (MOMDP) framework. Our contributions are multi-fold. First, as our transition model, we generalize the celebrated Susceptible-Infected-Removal (SIR) model (Kermack and McKendrick 1927) to allow simultaneous estimation of the infectious ability of this disease and evaluation for the effectiveness of different control measures, in an online fashion. There is a vast literature on modeling and prediction for infectious diseases; see (Keeling and Rohani 2011) for an overview. Among these work, compartmental models such as the SIR model are widely used; see, e.g., (Song et al. 2020) and (Sun et al. 2020) for applications to COVID-19. During an outbreak, the knowledge about the infectious ability and the effectiveness of interventions usually change a lot, and a quantitative decision making support tool should utilize the update-to-date information timely. However, none of these works considers

online parameter updating and intervention effect estimation at the same time. We aim to achieve this goal via an online Bayesian framework.

Second, we propose a novel online planning framework to assist policymakers in making decisions to minimize the overall long-term cost. In reality, policymakers generally group different interventions into several ordered levels with increasing strictness and then choose among them (e.g., states in the U.S. (Korevaar et al. 2020) and New Zealand (Wilson 2020)). This paper will focus on selecting among such a set of ordinal actions. Specifically, at each decision point, on the ground of the estimated generalized SIR model, we propose a model-based planning algorithm to find the optimal intervention policy among an interpretable class, for each given weight between the two competing objectives, the epidemiological cost and the economic cost. We then extend the algorithm to obtain a representative set of Pareto-optimal policies, i.e., policies that cannot be improved for one objective without sacrificing another. This framework, combined with the prediction bands for each policy, achieves the goal of supporting multi-objective decision making. Compared with the huge literature on infectious disease modeling and prediction, the optimal decision-making problem is much less studied. Most works either focus on the evaluation of several fixed interventions (Tildesley et al. 2006; Ferguson et al. 2020; Hellewell et al. 2020) or study the optimal control problem with a deterministic model (Ledzewicz and Schättler 2011; Elhia, Rachik, and Benlahmar 2013). None of these works allows sequential decision making with online updated parameter estimation, which enables selecting the appropriate intervention according to the current state and available data. In addition, the long-term effect is particularly important in this application due to the spread nature of the pandemic. Reinforcement learning (RL) is particularly suitable for these purposes, while its application in infectious disease control is relatively new to the literature. The existing works (e.g., (Probert et al. 2018), (Laber et al. 2018), (Zlojutro, Rey, and Gardner 2019), etc.) are mainly concerned with the problem caused by limited resources. In contrast, we focus on another aspect, the multi-objective problem caused by the huge costs of stringent control measures. This approach provides us with a clearer view of the trade-off. To our knowledge, this is the first work about applications of multi-objective RL to infectious disease control.

Third, an application of our method to control the outbreak of COVID-19 in China is presented as an example. This application is important in its own right. Our proposed framework is generally applicable to infectious disease pandemics.

Related work. In addition to the literature on infectious disease-related modeling, prediction, and decision making, our methodology also belongs to the field of reinforcement learning. Our problem is closely related to the line of research on MOMDPs (see (Roijers et al. 2013) or (Liu, Xu, and Hu 2014) for a survey), which studies problems with multiple competing objectives. When the weight between objectives is unknown, the literature focuses on approximately obtaining the whole class of Pareto-optimal policies (Castelletti, Pianosi, and Restelli 2012; Barrett and Narayanan 2008; Parisi, Pirotta, and Peters 2017; Pirotta, Parisi, and Restelli 2015). Because of the online planning nature in our case, it suffices to adopt a simpler approach, by performing multiple runs of policy search over a representative set of weights (Van Moffaert, Drugan, and Nowé 2013; Natarajan and Tadepalli 2005). Besides, RL algorithms are commonly classified as model-based methods (e.g., MBVE (Feinberg et al. 2018), MCTS (Browne et al. 2012), etc.), which directly learn a model of the system dynamics, and model-free methods (e.g., fitted-Q iteration (Riedmiller 2005), deep-Q network (Mnih et al. 2015), actor-critic (Konda and Tsitsiklis 2000), etc.), which do not. In the case of emerging infectious disease control, on one hand, the algorithm needs to generalize to unseen transitions (e.g., the end of the epidemic), where the model-free approach is typically not applicable (van Hasselt, Hessel, and Aslanides 2019); on the other hand, some epidemiological models have demonstrated satisfactory prediction power. Therefore, the model-based approach is adopted in this paper. Finally, we note that some efforts have been made in the literature to study the optimal control policy for COVID-19 (Alvarez, Argente, and Lippi 2020; Piguillem and Shi 2020; Eftekhari et al. 2020). As discussed above, these works did not consider the multi-objective problem but assigned a fixed price for each life to scalarize the objective, and in addition, they focus on solving a one-time planning problem to decide all future actions instead of providing a real-time decision-making framework.

Outline. The remainder of this paper is structured as follows: we first outline the proposed decision making workflow in Section 2, and then discuss the details of several components in Section 3. The numerical experiments and results are presented in Section 4. We conclude the paper with discussions and possible extensions in Section 5.

2 Framework of the Multi-Objective Decision Support Tool

2.1 Preliminaries

A Markov decision process (MDP) is a sequential decision making model which can be represented by a tuple $\langle \mathcal{S}, \mathcal{A}, c, f \rangle$, where \mathcal{S} is the state space, \mathcal{A} is the action space, $c : \mathcal{S} \times \mathcal{A} \rightarrow \mathbb{R}$ is the expected cost function, and $f : \mathcal{S}^2 \times \mathcal{A} \rightarrow \mathbb{R}$ is a Markov transition kernel. Throughout the paper we use *cost* instead of *reward*. A multi-objective MDP (MOMDP) is an extension of the MDP model when there are several competing objectives. An MOMDP can be represented as a tuple $\langle \mathcal{S}, \mathcal{A}, \mathbf{c}, f \rangle$, where the other components are defined as above and $\mathbf{c} = (c^1, \dots, c^K)^T$ is a vector of K cost functions for K different objectives, respectively.

In this paper, we consider the finite horizon setting with a pre-specified horizon T , which can simply be selected as a large enough number without loss of generality, since the costs we consider will be close to zero after the disease being controlled. In addition, we will focus on deterministic policies for realistic consideration. For a deterministic policy π , we define its k -th value function at time t_0 as $V_{k,t_0}^\pi(s) = \mathbb{E}_\pi(\sum_{t=t_0}^T c^k(S_t, A_t) | S_{t_0} = s)$, where \mathbb{E}_π denotes the expectation assuming $A_t = \pi(S_t)$ for every $t \geq t_0$. In the MDP setting, the objective is typically to find an optimal policy π^* that minimizes the expected cumulative cost among a policy class \mathcal{F} . However, in an MOMDP, there may not be a single policy that minimizes all costs. Instead, we consider the set of Pareto-optimal policies with linear preference functions $\Pi_{t_0} = \{\pi \in \mathcal{F} : \exists \omega \in \Omega \text{ s.t. } \omega^T \mathbf{V}_{t_0}^\pi(s) \leq \omega^T \mathbf{V}_{t_0}^{\pi'}(s), \forall \pi' \in \mathcal{F}, s \in \mathcal{S}\}$, where $\Omega = \{\omega \in \mathbb{R}_+^K : \omega^T \mathbf{1} = 1\}$ and $\mathbf{V}_{t_0}^\pi = (V_{1,t_0}^\pi, \dots, V_{K,t_0}^\pi)^T$. A policy is called Pareto-optimal if it can not be improved for one objective without sacrificing the others. The dependency on t_0 is to be consistent with the online planning setting considered in this paper.

2.2 The generalized SIR model

The SIR model is one of the most widely applied models to describe the dynamics of infectious diseases (Brauer 2008). Suppose at time t , the infectious disease is spread within N_t regions. Denote the total population of the l -th region as M_l , for $l = 1, \dots, N_t$. With the SIR model, we divide the total population into three groups: the individuals who can infect others, who have been removed from the infection system, and who have not been infected and are still susceptible. Denote the count for each group in region l at time t as $X_{l,t}^I$, $X_{l,t}^R$, and $X_{l,t}^S = M_l - X_{l,t}^I - X_{l,t}^R$, respectively. We will discuss how to construct these variables using observational data in Section 3.1. The standard deterministic SIR model can then be written as a system of difference equations:

$$\begin{aligned} X_{l,t+1}^S &= X_{l,t}^S - \beta X_{l,t}^S X_{l,t}^I / M_l; \\ X_{l,t+1}^I &= X_{l,t}^I + \beta X_{l,t}^S X_{l,t}^I / M_l - \gamma X_{l,t}^I; \\ X_{l,t+1}^R &= X_{l,t}^R + \gamma X_{l,t}^I, \end{aligned}$$

where β and γ are constants representing the infection and removal rate, respectively.

There are two limitations with the above SIR model. First, the infection rate heavily depends on the control measure being taken. As discussed in Section 1, in this paper we focus on an ordinal set of actions $\mathcal{A} = \{1, 2, \dots, J\}$, with level 1 standing for no official measures. Second, a stochastic model with proper distribution assumptions is required to fit real data with randomness. Motivated by the discussions above, we propose the generalized SIR (GSIR) model and use it as our **transition model**:

$$\begin{aligned} X_{l,t+1}^S &= X_{l,t}^S - e_{l,t}^S, \quad e_{l,t}^S \sim \text{Poisson}(\sum_{j=1}^J \beta_j \mathbb{I}(A_{l,t} = j) X_{l,t}^S \frac{X_{l,t}^I}{M_l}); \\ X_{l,t+1}^R &= X_{l,t}^R + e_{l,t}^R, \quad e_{l,t}^R \sim \text{Binomial}(X_{l,t}^I, \gamma); \\ X_{l,t+1}^I &= M_l - X_{l,t+1}^S - X_{l,t+1}^R, \end{aligned} \tag{1}$$

where $\mathbb{I}(\cdot)$ is the indicator function, $A_{l,t}$ is the action taken by region l at time t , and β_j denotes the infection rate under action j . We assume $\beta_1 \geq \beta_2 \geq \dots \geq \beta_J \geq 0$ to represent the increasing effectiveness. The estimation of $\theta = (\gamma, \beta_1, \dots, \beta_J)^T$ is deferred to Section 3.2.

2.3 Sequential decision making

In this work, we focus on the intervention decision of each region: in the model estimation step, data from several similar regions are aggregated together to share information and mediate the issue that

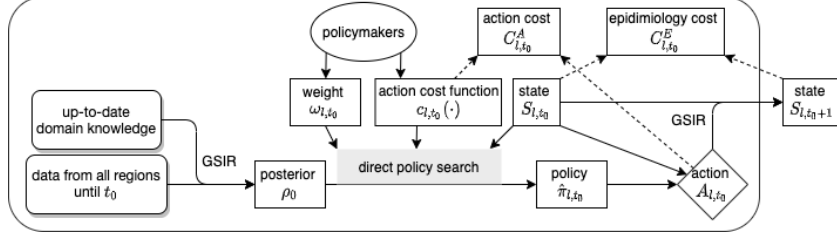


Figure 1: Decision making process for region l at time t_0

data is typically noisy, scarce, and single-episode in a pandemic; while in the decision making step, each region chooses its own action.

MOMDP definition. The intervention decision making problem can be naturally formalized as an MOMDP. For each region l , at each decision point t , according to the estimated transition model, the current **state** $S_{l,t} = (X_{l,t}^S, X_{l,t}^I, X_{l,t}^R)^T$, and their judgment, the policymakers determine a **policy** $\pi_{l,t}$ with the objective of minimizing the overall long-term cost, and choose the **action** $A_{l,t}$ to implement according to the policy. This action, assuming being effectively executed, will affect the infection rate during $(t, t+1]$ and hence the conditional distribution of $S_{l,t+1}$. Let $f(\cdot|\cdot, \cdot; \theta)$ be the conditional density for $S_{l,t+1}$ given $S_{l,t}$ and $A_{l,t}$ in model (1). In this work, we consider two cost variables, the **epidemiological cost** $C_{l,t}^E$ and the **action cost** $C_{l,t}^A$. $C_{l,t}^E$ can be naturally chosen as the number of new infections $X_{l,t}^S - X_{l,t+1}^S$. Let $C_{l,t}^A = c_l(Z_{l,t}, A_{l,t}, Z_{l,t+1}) \in \mathbb{R}^+$ for a time-varying variable $Z_{l,t}$ and a stochastic function c_l . Both c_l and $Z_{l,t}$ should be chosen by domain experts. For example, with $Z_{l,t}$ representing the unemployment rate, $C_{l,t}^A = Z_{l,t+1} - Z_{l,t}$ can represent its change due to $A_{l,t}$. Since the modeling for action cost and its transition is a separate question, for simplicity, we focus on the case that $C_{l,t}^A = c_l(A_{l,t})$ for a pre-specified stochastic function $c_l(\cdot)$ in this paper. $c_l(\cdot)$ is set to be region-specific to incorporate local features, such as the economic conditions. With a given weight $\omega_{l,t} \in \mathbb{R}^+$, the **overall cost** $C_{l,t}$ is then defined as $C_{l,t}^E + \omega_{l,t} C_{l,t}^A$. The expected cost functions can then be derived from these definitions, and for decision-making purposes, the overall cost is equivalent with the weighted cost defined in Section 2.1 when $K = 2$.

Online planning. For each region l , the online planning workflow is described as follows. We consider a sequence of decision points $\mathcal{T} \subset \{1, \dots, T\}$ to reduce the action switch cost in real applications. At time $t_0 \notin \mathcal{T}$, the region keeps the same action with time $t_0 - 1$. At time $t_0 \in \mathcal{T}$, the policymakers choose an action according to the decision making workflow displayed in Figure 1, which is summarized as follows: we first estimate the posterior of θ as ρ_{t_0} , using accumulated data $\mathcal{D}_{t_0} = \{S_{l,t}, A_{l,t}\}_{1 \leq l \leq N_{t_0}, 1 \leq t \leq t_0-1} \cup \{S_{l,t_0}\}_{1 \leq l \leq N_{t_0}}$ and priors selected with domain knowledge. The Bayesian approach is proffered here because (i) typically there is important domain knowledge available, (ii) we need to make decisions before accumulating sufficient data, and (iii) the model uncertainty should be emphasized in this case. Next, the policymakers choose the trade-off weight ω_{l,t_0} , learn a deterministic policy $\hat{\pi}_{l,t_0}(\cdot; \omega_{l,t_0})$ by planning, and implement $A_{l,t_0} = \hat{\pi}_{l,t_0}(S_{l,t_0}; \omega_{l,t_0})$. Formally, we solve the following optimization problem to obtain $\hat{\pi}_{l,t_0}(\cdot; \omega_{l,t_0})$:

$$\hat{\pi}_{l,t_0}(\cdot; \omega_{l,t_0}) = \underset{\pi \in \mathcal{F}}{\operatorname{argmin}} \mathbb{E}_{\pi, \rho_{t_0}} \left(\sum_{t=t_0}^T (C_{l,t}^E + \omega_{l,t_0} C_{l,t}^A) \right), \quad (2)$$

where $\mathbb{E}_{\pi, \rho_{t_0}}$ denotes the expectation assuming $C_{l,t}^A \sim c_l(A_{l,t})$, $\mathbb{P}(S_{l,t+1} = s_{l,t+1} | S_{l,t} = s_{l,t}, A_{l,t} = a_{l,t}) = f(s_{l,t+1} | s_{l,t}, a_{l,t}; \theta)$ with $\theta \sim \rho_{t_0}$, and $A_{l,t} = \pi(S_{l,t})\mathbb{I}(t \in \mathcal{T}) + A_{l,t-1}, \mathbb{I}(t \notin \mathcal{T})$, for every $t \geq t_0$. The specification of \mathcal{F} and the policy search algorithm for solving (2) will be discussed in Section 3.3.

2.4 Multiple objectives and the Pareto-optimal policies

In the discussion above, we assume the tradeoff weight ω_{l,t_0} is easily specified at each decision point. This is feasible when the two objectives share the same unit, for example, when $C_{l,t}^A$ represents the damage to public health due to economic losses. In general settings, properly choosing the weight is not easy and sometimes unrealistic. Therefore, we aim to assemble a decision support tool that

provides a comprehensive picture of the future possibilities associated with different weight choices and hence makes the multi-objective decision making feasible.

Solving the whole set of Pareto-optimal policies is typically quite challenging. While in our online planning setting, for each decision point t_0 , we only need to make a one-time decision among a few available actions. For this purpose, it is not necessary to generate all such policies. We can simply solve problem (2) for a representative set of weights $\{\omega_b\}_{b=1}^B$ to find the corresponding Pareto-optimal policies, and then apply Monte Carlo simulation to obtain the corresponding prediction bands for the potential costs following each policy. The policymakers can then compare all these possible trajectories, select among them, and hence choose the action A_{l,t_0} . We summarize this tool in Algorithm 1.

Algorithm 1: Pareto-optimal Policies and Prediction Bands

Input: weights $\{\omega_b\}_{b=1}^B$, number of replications K , significance level α , action cost function $c_l(\cdot)$, decision points $\mathcal{T}, \mathcal{D}_{t_0}, \rho_{t_0}, T$.

for $b = 1, \dots, B$ **do**

 apply a policy search algorithm (e.g., Algorithm 3) to find the optimal policy $\hat{\pi}^b$ for weight ω_b .

for $k = 1, \dots, K$ **do**

 set the cumulative cost $V_{t_0-1}^{k,E}$ and $V_{t_0-1}^{k,A}$ as 0

 set $S_{t_0,b}^k = S_{t_0}$

for $t = t_0, \dots, T$ **do**

 choose action $A_{t,b}^k = \hat{\pi}^b(S_{t,b}^k)\mathbb{I}(t \in \mathcal{T}) + A_{t-1,b}^k\mathbb{I}(t \notin \mathcal{T})$

 sample $C_{t,b}^{k,A} \sim c_l(A_{t,b}^k)$, $\theta_{t,b}^k \sim \rho_{t_0}$, and $S_{t+1,b}^k \sim f(\cdot | S_{t,b}^k, A_{t,b}^k; \theta_{t,b}^k)$

 calculate $V_{t,b}^{k,E} = V_{t-1,b}^{k,E} + X_{t,b}^{k,S} - X_{t+1,b}^{k,S}$ and $V_{t,b}^{k,A} = V_{t-1,b}^{k,A} + C_{t,b}^{k,A}$

for $t \in \{t_0, \dots, T\}$, calculate the upper and lower $\alpha/2$ -th quantile and the mean of $\{V_{t,b}^{k,E}\}_{k=1}^K$ as $V_{u,t}^{b,E}$, $V_{l,t}^{b,E}$, and $\bar{V}_t^{b,E}$, respectively; similarly calculate $V_{u,t}^{b,A}$, $V_{l,t}^{b,A}$, and $\bar{V}_t^{b,A}$.

Result: optimal policies $\{\hat{\pi}^b\}_{b=1}^B$, recommended actions $\{A_{t_0,b}^1\}_{b=1}^B$, prediction bands for costs $\{ \{ (V_{l,t}^{b,E}, V_{u,t}^{b,E}, \bar{V}_t^{b,E}), (V_{l,t}^{b,A}, V_{u,t}^{b,A}, \bar{V}_t^{b,A}) \}_{t=t_0}^T \}_{b=1}^B$

3 Details of the Decision Support Tool

3.1 State construction

In this section, we discuss how to construct the state variables with surveillance data. The data usually available to policymakers is the cumulative count of confirmed cases until time t , denoted as $O_{l,t}^I$. We can naturally set $X_{l,t}^R$ as $O_{l,t}^I$, since the individuals counted in $O_{l,t}^I$ generally either have been confirmed and isolated, or have recovered or died. For infectious diseases, there is typically a time delay between being infectious and getting isolated, the length of which is treated as a random variable with expectation D . Therefore, the count of the infectious $X_{l,t}^I$ is usually not immediately observable at time t , but will be gradually identified in the following days. Following the existing works on infectious disease modelling (Zhang et al. 2005; Chen et al. 2020), we treat this issue as a delayed observation problem and use $O_{l,t+D}^I - O_{l,t}^I$, the new confirmed cases during $(t, t+D]$, as a proxy for $X_{l,t}^I$. In the planning step, following the literature on delayed MDPs (Walsh et al. 2009), we apply Algorithm 2 (Model-based Simulation, MBS) to generate a belief state, and then choose the action according to it. We note that although this issue is not obvious in prediction, it is unavoidable in decision making because $A_{l,t}$ works directly on $X_{l,t}^I$. It also reminds us that our control decisions should be based on the latent state instead of only the confirmed cases. The performance of such an approximation is examined with numerical experiments in Section 4.

3.2 Estimation of the transition model

At each time $t_0 \in \mathcal{T}$, we need to first obtain the posterior of θ in the transition model (1). Notice that the last equation in (1) is redundant under the constraint $X_{l,t}^S + X_{l,t}^I + X_{l,t}^R = M_l$ for all t . With

Algorithm 2: Model-based Simulation (MBS)

Data: $\{O_{l,t}^I\}_{t=t_0-D}^{t_0}$, $\{A_{l,t}\}_{t=t_0-D}^{t_0-1}$, ρ_{t_0} , and D
set $X_{l,t_0-D}^{I,G} = O_{l,t_0}^I - O_{l,t_0-D}^I$ and $(\hat{\gamma}_{t_0}, \hat{\beta}_{1,t_0}, \dots, \hat{\beta}_{J,t_0})^T = \mathbb{E}(\rho_{t_0})$.
for $t = t_0 - D, \dots, t_0 - 1$ **do**
 $X_{l,t+1}^{I,G} = X_{l,t}^{I,G} + \sum_{j=1}^J \hat{\beta}_{j,t_0} \mathbb{I}_{\{A_{l,t}=j\}} (M_l - O_{l,t}^I - X_{l,t}^{I,G}) X_{l,t}^{I,G} / M_l - (O_{l,t+1}^I - O_{l,t}^I)$
Result: the belief state $S_{l,t_0} = (M_l - X_{l,t_0}^{I,G} - O_{l,t_0}^I, X_{l,t_0}^{I,G}, O_{l,t_0}^I)^T$

data \mathcal{D}_{t_0} , the Markov property reduces the estimation problem to $J + 1$ Bayesian generalized linear models with the identity link function. With proper choices of the conjugate priors, the posterior distributions have explicit forms. To save space, we postpone the derivations to Section A in the supplement.

Below, we introduce a way to specify the prior parameters: (i) β_1 and γ are both features of this disease without any interventions, and we can first set their priors with the estimates of similar diseases, and update them when additional biochemical findings are available; (ii) for $j \geq 2$, β_j indicates the infection rate under action level j . Suppose we have a reasonable estimate of the intervention effect $u_j = \beta_j / \beta_1$ as \hat{u}_j and that of β_1 as $\hat{\beta}_1$, then the prior of β_j can be set as a distribution with expectation $\hat{u}_j \hat{\beta}_1$.

3.3 Policy search

At each decision point $t_0 \in \mathcal{T}$, for each region l and a given weight ω_{l,t_0} , we need to find the optimal policy $\hat{\pi}_{l,t_0}(\cdot; \omega_{l,t_0}) \in \mathcal{F}$ by solving the model-based planning problem (2). \mathcal{F} is supposed to be a general and interpretable policy class, since interpretability is of great importance in this application. In this work, we focus on the following observations from the pandemic control decision making process in real life: (i) the decision should be based on the spread severity, which we interpret as $X_{l,t}^I$, the number of infectious individuals; (ii) the policy should also be based on the current estimate of disease features ρ_{t_0} , the current state S_{l,t_0} , the trade-off weight ω_{l,t_0} , and the potential cost $c_l(\cdot)$, which have all been incorporated in the objective function of (2); (iii) the more serious the situation, the more stringent the intervention should be. Motivated by these observations, we consider the following policy class:

$$\mathcal{F} = \{\pi : \pi(S_{l,t}; \boldsymbol{\lambda}) = \sum_{j=1}^J j \mathbb{I}(\lambda_j \leq X_{l,t}^I < \lambda_{j+1}), \\ 0 = \lambda_1 \leq \lambda_2 \leq \dots \leq \lambda_{J+1} = M_l, \lambda_J \leq \lambda_M\},$$

where $\boldsymbol{\lambda} = (\lambda_2, \dots, \lambda_J)^T$. Notice that $X_{l,t}^I$ is generally a number much smaller than M_l , we introduce the pre-specified tolerance parameter $\lambda_M \in (0, M_l)$ to reduce the computational cost by deleting unrealistic policies.

In this paper, we use the rollout-based direct policy search to solve Problem (2). Direct policy search algorithms generally apply optimization algorithms to maximize the value function approximated via Monte Carlo rollouts (Gosavi et al. 2015). Since the state transition and the action cost are both computationally affordable to sample in our case, when J is not large, we can simply apply the grid search algorithm to efficiently and robustly find the optimal policy. The example for $J = 3$, which is the case in our experiment, is described in Algorithm 3. When J is large, many other optimization algorithms can be used and a simultaneous perturbation stochastic approximation algorithm (Sadeh 1997) is provided in Section B.1 of the supplement. The computational complexity of our algorithm is discussed in Section B.2 of the supplement.

4 Application to COVID-19

In this section, we apply our framework to some COVID-19 data in China for illustration. China has passed the first peak, which provides data with good quality for validation purposes. Moreover,

Algorithm 3: Policy Search with Grid Search

Input: bounds of the search space u_2, u_3, U_2, U_3 ; step sizes ξ_2, ξ_3 ; number of replications M ; data $\{O_{l,t}^I\}_{t=t_0-D}^{t_0}$ and $\{A_{l,t}\}_{t=t_0-D}^{t_0-1}$; other parameters $D, \rho_{t_0}, w_{l,t_0}, t_0, T, \mathcal{T}, c_l(\cdot)$

set $\lambda_2 = u_2, V^* = +\infty, S_{l,t_0} = MBS(\{X_{l,t}^R\}_{t=t_0-D}^{t_0}, \{A_{l,t}\}_{t=t_0-D}^{t_0-1}, \rho_{t_0}, D)$, and $X_{l,t}^R = O_{l,t}^I$ for $t \in \{t_0 - D, \dots, t_0\}$

while $\lambda_2 \leq U_2$ **do**

 set $\lambda_3 = \max(\lambda_2, u_3)$

while $\lambda_3 \leq U_3$ **do**

 set $\lambda = (\lambda_2, \lambda_3)^T$ and the overall value $V = 0$

for $m = 1, \dots, M$ **do**

for $t' = t_0, \dots, T$ **do**

 generate $S_{l,t'}^G = MBS(\{X_{l,t'}^R\}_{t=t'-D}^{t'}, \{A_{l,t'}\}_{t=t'-D}^{t'-1}, \rho_{t_0}, D)$

 choose action $A_{l,t'} = \pi(S_{l,t'}^G; \lambda) \mathbb{I}(t' \in \mathcal{T}) + A_{l,t'-1} \mathbb{I}(t' \notin \mathcal{T})$

 sample $\theta \sim \rho_{t_0}, C_{l,t'}^A \sim c_l(A_{l,t'})$, and $S_{l,t'+1} \sim f(\cdot | S_{l,t'}, A_{l,t'}; \theta)$

 calculate $V = V + (X_{l,t'}^S - X_{l,t'+1}^S + w_{l,t_0} C_{l,t'}^A)$

if $V < V^*$ **then** update $V^* = V$ and $\lambda^* = \lambda$

 set $\lambda_3 = \lambda_3 + \xi_3$

 set $\lambda_2 = \lambda_2 + \xi_2$

Output: optimal policy $\hat{\pi}_{l,t_0}(\cdot; w_{l,t_0}) = \pi(\cdot; \lambda^*)$

COVID-19 is still spreading worldwide, and we hope this framework can provide some informative suggestions to regions in the COVID-19 cycle.

4.1 Data description and hyper-parameters

We collect data for six important cities in China from 01/15/2020 to 05/13/2020, and index these cities by $l \in \{1, \dots, 6\}$ and dates by $t \in \{1, \dots, 120\}$, with $T = 120$. More details about the dataset and hyper-parameters can be found in Section C.1 in the supplement.

State variables and region-specific features: the counts of confirmed cases for each city are collected from (Lab 2020). For each region l , we collect its annual gross domestic product (GDP) G_l and population M_l from a Chinese demographic dataset¹.

Action: three levels of intervention measures implemented in China during COVID-19 are considered and data are collected from the news: level 1 means no or few official policies claimed; level 2 means the public health emergency response; level 3 means the stringent closed-off management required by the government.

Cost: we use $r_{l,t}$, the observed ratio of human mobility loss in city l on day t compared with year 2019, to construct a proxy for its GDP loss and calibrate the action cost function $c_l(\cdot)$. The data is collected from the online platform Baidu Migration² and it is collected until day 61 due to availability. we first fit a normal distribution $\mathcal{N}(\mu_j, \sigma_j^2)$ to $\{r_{l,t} | A_{l,t} = j, 1 \leq l \leq 6, 1 \leq t \leq 61\}$ for $j \in \{2, 3\}$, and then define $c_l(a)$ as $\sum_{j=1}^3 C_j \mathbb{I}(a = j) G_l / 365$, where $C_1 = 0$ and $C_j \sim \mathcal{N}(\mu_j, \sigma_j^2)$ for $j \in \{2, 3\}$. We note that this is only for illustration purposes. In real applications, policymakers need to carefully design and measure the potential costs with domain experts.

Hyper-parameters: the parameter estimates for a similar pandemic SARS (Mkhatshwa and Mumert 2010) are used as priors of γ and β_1 . Similar to (Ferguson et al. 2020), we assume that action 2 and 3 can reduce the infection rate by 80% and 90%, respectively, and set the priors for β_2 and β_3 accordingly. D is chosen as 9 according to (Sun et al. 2020) and (Pellis et al. 2020). All the above hyper-parameters are chosen according to domain knowledge, and sensitivity analysis provided in the supplement show that the performance is robust.

¹<https://www.hongheiku.com>

²<http://qianxi.baidu.com>

4.2 Estimation and validation of the transition model

The performance of our learned policies and the choices of weights both rely on the prediction accuracy of the estimated GSIR model, and we aim to examine this point via temporal validation. Specifically, We first estimate the GSIR model using all data until day 12, and then for each city l , we predict $X_{l,t}^R$, the count of cumulative confirmed cases, from day 13 to 120 following the observed actions in data via forward sampling with the estimated GSIR model. The results over 1000 replications are plotted in Figure 2 and the prediction bands successfully cover the observed counts in most cases.

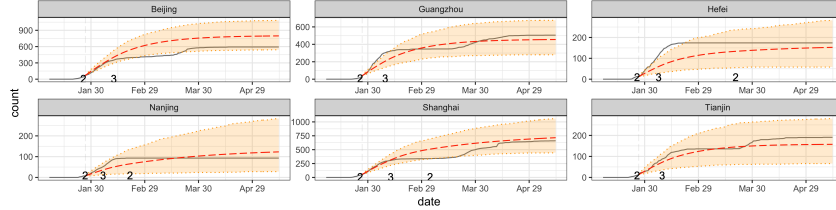


Figure 2: Validation results for the six important cities in China. The solid lines are the observed counts of the cumulative infected cases, and the red dotted lines represent the mean predicted numbers. The shaded areas indicate the 99% prediction bands. When a different action was taken, we annotate the new action level on the change point.

To provide more insights into the intervention effects, in Table 1, we present the estimated parameters using all data until day 61, since the new cases afterwards are sparse. Here, $R_0^j = \beta_j / \gamma$ is the basic reproduction number under action level j , which plays an essential role in epidemiology analysis (Delamater et al. 2019). Roughly speaking, $R_0^j < 1$ implies the pandemic will gradually diminish under action j . The small value of R_0^3 indicates that action 3 has a significant effect on controlling the pandemic; measure 2 is also effective and is more like a mitigation strategy; the estimate of R_0^1 is consistent with the existing results (Alimohamadi, Taghdir, and Sepandi 2020), and it emphasizes that a lack of intervention will lead to a disaster. We also reported the estimates used to make the predictions in Figure 2. Although the estimation is not perfect due to data scarcity in the early stage, the prediction still captures the rough trend under a reasonable policy and we expect it will not affect the decision making significantly.

Table 1: The posterior means and standard deviations (in the parentheses) obtained using data for all the six cities until day t_0 .

t_0	R_0^1	R_0^2	R_0^3	γ	β_1	β_2	β_3
12	4.13 (.34)	0.74 (.09)	0.37 (.06)	0.07 (.005)	0.29 (.011)	0.05 (.005)	0.03 (.004)
61	2.32 (.09)	0.70 (.03)	0.38 (.03)	0.11 (.002)	0.25 (.007)	0.07 (.003)	0.04 (.003)

4.3 Evaluation of the Pareto-optimal policies

In this section, we conduct a simulation experiment to compare the performance of our proposed method with several competing policies on curbing the spread of COVID-19. Specifically, for the six cities, we start from day 12 together and follow the actions recommended by a specific policy until day 120, with the cumulative costs recorded. The state transitions are generated from the GSIR model with $\mathbb{E}(\rho_{61})$ as the parameter, and the observations before day 12 are kept the same with the real data. The validity of $\mathbb{E}(\rho_{61})$ as the environment parameter is examined via cross-validation in Section C.2 in the supplement.

Motivated by the real life observations and the candidate policies considered in the literature (Merl et al. 2009; Lin, Muthuraman, and Lawley 2010; Ludkovski and Niemi 2010), we make comparisons among the following policies:

1. Our proposed Pareto-optimal policies π_k for $k \in \{-2, 0, \dots, 6\}$: we fix the weight as $e^k/10$ across all cities and time, and follow the workflow proposed in Section 2.3. \mathcal{T} is set as every seven days.

2. Occurrence-based mitigation policy π_m^M for $m \in \{4, 6, \dots, 12\}$: a city implements action 2 when there are new cases confirmed in the past m days, and action 1 otherwise.
3. Occurrence-based suppression policy π_m^S for $m \in \{4, 6, \dots, 10\}$: a city begins to implement action 2 after m days from its first confirmed case and strengthens it to level 3 after m more days. Afterwards, the city weakens the action to level 2 when there have been no new cases for m days and level 1 for $2m$ days.
4. Count threshold-based policy π_m^{TB} for $m \in \{5, 10, \dots, 50\}$: a city implements action 3 when the count of new cases on the day before exceeds m , action 1 when it is zero, and action 2 otherwise.
5. Behaviour policy π^B : the observed trajectories in the dataset.

We run experiments on a c5d.24xlarge instance on the AWS EC2 platform, with 96 cores and 192GB RAM, and it takes roughly 6 hours to complete. For each policy except for π^B , we run 100 replications and present the average costs in Figure 3. The standard errors are small and reported in the supplement. We can see that the proposed method provides a clear view of the tradeoff between the two objectives and its performance is generally better than the competing policies. The behaviour policy by Chinese local governments is quite strict in the later period, and we interpret part of this effort as the attempt to curb the cross-border spread. The other policies are not Pareto-optimal and also are not adaptive to different situations in different cities. The clear trend among the occurrence-based suppression policies emphasizes the importance of intervening as promptly as possible, which can reduce both costs.

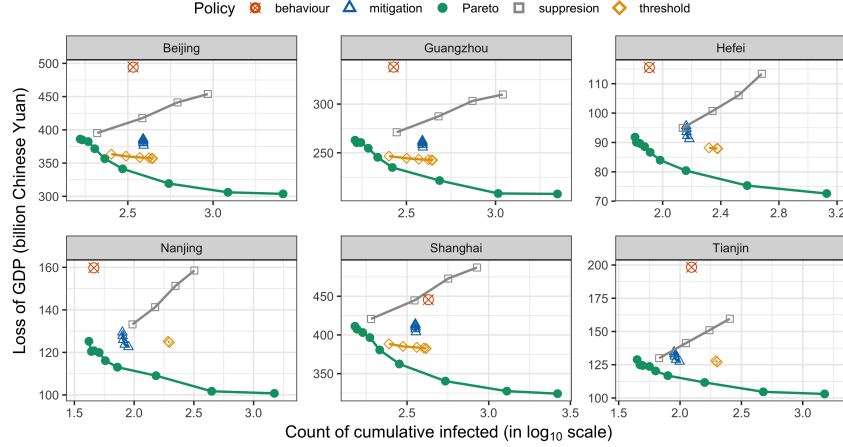


Figure 3: Cumulative epidemiological costs and economic costs following different policies, averaged over 100 replications. The closer to the left bottom corner, the better.

5 Discussion

This work is motivated by the ongoing COVID-19 pandemic, where it is witnessed that the decision making can be impeded by the huge intervention costs and the uncertainty. We propose a novel model-based multi-objective reinforcement learning framework to assist policymakers in real-time decision making with the objective of minimizing the overall long-term cost. The method shows promising performance in numerical studies.

The overall framework is generally applicable to infectious disease pandemics and there are several components that can be extended: (i) other epidemiology models than the SIR model can also be used as the transition model, with the estimation method and policy class modified correspondingly; (ii) more than two objectives can be similarly formalized and resource limits can also be considered by including constraints in the specification of the policy class; (iii) other policy classes can be similarly formalized depending on the information required for decision making. As future directions, the spreads among multiple regions can be incorporated under the multi-agent reinforcement learning framework, the partially observable MDPs can be considered to deal with the delayed observation

problem, and a multidimensional action space with the combinations of different interventions is a meaningful next step.

Ethics Statement

We would like to emphasize that taking the economy as more important than human lives is not a motivation or an outcome of this framework. On one hand, economic losses can also cause health damage to many people, probably not less than the direct damage from the disease; on the other hand, the estimated Pareto-optimal policies aim to help policymakers reduce the cost on one objective without sacrificing the other, as illustrated in Section 4.3.

The framework is designed with the overall welfare of all people in mind. We acknowledge that the degree of interest loss for different groups may vary due to different choices among the Pareto-optimal policies, which is a tricky and unavoidable ethical question. For this purpose, an online interactive tool and an open-sourced software are under development to facilitate the real-time dissemination of results. Everybody is welcome to utilize these tools to have a better understanding of the current situation and participates in the discussion.

References

- Alimohamadi, Y.; Taghdir, M.; and Sepandi, M. 2020. The estimate of the basic reproduction number for novel coronavirus disease (COVID-19): a systematic review and meta-analysis. *Journal of Preventive Medicine and Public Health*.
- Alvarez, F. E.; Argente, D.; and Lippi, F. 2020. A simple planning problem for covid-19 lockdown. Technical report, National Bureau of Economic Research.
- Anderson, R. M.; Heesterbeek, H.; Klinkenberg, D.; and Hollingsworth, T. D. 2020. How will country-based mitigation measures influence the course of the COVID-19 epidemic? *The Lancet* 395(10228): 931–934.
- Barrett, L.; and Narayanan, S. 2008. Learning all optimal policies with multiple criteria. In *Proceedings of the 25th international conference on Machine learning*, 41–47.
- Brauer, F. 2008. Compartmental models in epidemiology. In *Mathematical epidemiology*, 19–79. Springer.
- Browne, C. B.; Powley, E.; Whitehouse, D.; Lucas, S. M.; Cowling, P. I.; Rohlfshagen, P.; Tavener, S.; Perez, D.; Samothrakakis, S.; and Colton, S. 2012. A survey of monte carlo tree search methods. *IEEE Transactions on Computational Intelligence and AI in games* 4(1): 1–43.
- Castelletti, A.; Pianosi, F.; and Restelli, M. 2012. Tree-based fitted Q-iteration for multi-objective Markov decision problems. In *The 2012 International Joint Conference on Neural Networks (IJCNN)*, 1–8. IEEE.
- Chen, B.; Shi, M.; Ni, X.; Ruan, L.; Jiang, H.; Yao, H.; Wang, M.; Song, Z.; Zhou, Q.; and Ge, T. 2020. Data Visualization Analysis and Simulation Prediction for COVID-19. *arXiv preprint arXiv:2002.07096*.
- Delamater, P. L.; Street, E. J.; Leslie, T. F.; Yang, Y. T.; and Jacobsen, K. H. 2019. Complexity of the basic reproduction number (R_0). *Emerging infectious diseases* 25(1): 1.
- Eftekhari, H.; Mukherjee, D.; Banerjee, M.; and Ritov, Y. 2020. Markovian And Non-Markovian Processes with Active Decision Making Strategies For Addressing The COVID-19 Epidemic. *arXiv preprint arXiv:2008.00375*.
- Eichenbaum, M. S.; Rebelo, S.; and Trabandt, M. 2020. The macroeconomics of epidemics. Technical report, National Bureau of Economic Research.
- Elhia, M.; Rachik, M.; and Benlahmar, E. 2013. Optimal control of an SIR model with delay in state and control variables. *ISRN Biomathematics* 2013.

- Feinberg, V.; Wan, A.; Stoica, I.; Jordan, M. I.; Gonzalez, J. E.; and Levine, S. 2018. Model-based value estimation for efficient model-free reinforcement learning. *arXiv preprint arXiv:1803.00101* .
- Ferguson, N.; Laydon, D.; Nedjati-Gilani, G.; et al. 2020. Impact of non-pharmaceutical interventions (NPIs) to reduce COVID-19 mortality and healthcare demand. Imperial College COVID-19 Response Team.
- Gangopadhyaya, A.; and Garrett, A. B. 2020. Unemployment, Health Insurance, and the COVID-19 Recession. *Health Insurance, and the COVID-19 Recession (April 1, 2020)* .
- Gosavi, A.; et al. 2015. *Simulation-based optimization*. Springer.
- Hellewell, J.; Abbott, S.; Gimma, A.; Bosse, N. I.; Jarvis, C. I.; Russell, T. W.; Munday, J. D.; Kucharski, A. J.; Edmunds, W. J.; Sun, F.; et al. 2020. Feasibility of controlling COVID-19 outbreaks by isolation of cases and contacts. *The Lancet Global Health* .
- Keeling, M. J.; and Rohani, P. 2011. *Modeling infectious diseases in humans and animals*. Princeton University Press.
- Kermack, W. O.; and McKendrick, A. G. 1927. A contribution to the mathematical theory of epidemics. *Proceedings of the royal society of london. Series A, Containing papers of a mathematical and physical character* 115(772): 700–721.
- Konda, V. R.; and Tsitsiklis, J. N. 2000. Actor-critic algorithms. In *Advances in neural information processing systems*, 1008–1014.
- Korevaar, H. M.; Becker, A. D.; Miller, I. F.; Grenfell, B. T.; Metcalf, C. J. E.; and Mina, M. J. 2020. Quantifying the impact of US state non-pharmaceutical interventions on COVID-19 transmission. *medRxiv* .
- Lab, C. D. 2020. China COVID-19 Daily Cases with Basemap. doi:10.7910/DVN/MR5IJN. URL <https://doi.org/10.7910/DVN/MR5IJN>.
- Laber, E. B.; Meyer, N. J.; Reich, B. J.; Pacifici, K.; Collazo, J. A.; and Drake, J. M. 2018. Optimal treatment allocations in space and time for on-line control of an emerging infectious disease. *Journal of the Royal Statistical Society: Series C (Applied Statistics)* 67(4): 743–789.
- Ledzewicz, U.; and Schättler, H. 2011. On optimal singular controls for a general SIR-model with vaccination and treatment. *Discrete and continuous dynamical systems* 2: 981–990.
- Lin, F.; Muthuraman, K.; and Lawley, M. 2010. An optimal control theory approach to non-pharmaceutical interventions. *BMC infectious diseases* 10(1): 32.
- Liu, C.; Xu, X.; and Hu, D. 2014. Multiobjective reinforcement learning: A comprehensive overview. *IEEE Transactions on Systems, Man, and Cybernetics: Systems* 45(3): 385–398.
- Ludkovski, M.; and Niemi, J. 2010. Optimal dynamic policies for influenza management. *Statistical Communications in Infectious Diseases* 2(1).
- Merl, D.; Johnson, L. R.; Gramacy, R. B.; and Mangel, M. 2009. A statistical framework for the adaptive management of epidemiological interventions. *PloS One* 4(6): e5807.
- Mkhatshwa, T.; and Mummert, A. 2010. Modeling super-spreading events for infectious diseases: case study SARS. *arXiv preprint arXiv:1007.0908* .
- Mnih, V.; Kavukcuoglu, K.; Silver, D.; Rusu, A. A.; Veness, J.; Bellemare, M. G.; Graves, A.; Riedmiller, M.; Fidjeland, A. K.; Ostrovski, G.; et al. 2015. Human-level control through deep reinforcement learning. *Nature* 518(7540): 529–533.
- Natarajan, S.; and Tadepalli, P. 2005. Dynamic preferences in multi-criteria reinforcement learning. In *Proceedings of the 22nd international conference on Machine learning*, 601–608.
- Organization, W. H.; et al. 2020. Coronavirus disease 2019 (COVID-19): situation report, 72 .

- Parisi, S.; Pirotta, M.; and Peters, J. 2017. Manifold-based multi-objective policy search with sample reuse. *Neurocomputing* 263: 3–14.
- Pellis, L.; Scarabel, F.; Stage, H. B.; Overton, C. E.; Chappell, L. H.; Lythgoe, K. A.; Fearon, E.; Bennett, E.; Curran-Sebastian, J.; Das, R.; et al. 2020. Challenges in control of Covid-19: short doubling time and long delay to effect of interventions. *arXiv preprint arXiv:2004.00117*.
- Piguillem, F.; and Shi, L. 2020. Optimal COVID-19 quarantine and testing policies.
- Pirotta, M.; Parisi, S.; and Restelli, M. 2015. Multi-objective reinforcement learning with continuous pareto frontier approximation. In *Twenty-Ninth AAAI Conference on Artificial Intelligence*.
- Probert, W. J.; Jewell, C. P.; Werkman, M.; Fonnesebeck, C. J.; Goto, Y.; Runge, M. C.; Sekiguchi, S.; Shea, K.; Keeling, M. J.; Ferrari, M. J.; et al. 2018. Real-time decision-making during emergency disease outbreaks. *PLoS computational biology* 14(7): e1006202.
- Riedmiller, M. 2005. Neural fitted Q iteration—first experiences with a data efficient neural reinforcement learning method. In *European Conference on Machine Learning*, 317–328. Springer.
- Rojters, D. M.; Vamplew, P.; Whiteson, S.; and Dazeley, R. 2013. A survey of multi-objective sequential decision-making. *Journal of Artificial Intelligence Research* 48: 67–113.
- Sadegh, P. 1997. Constrained optimization via stochastic approximation with a simultaneous perturbation gradient approximation. *Automatica* 33(5): 889–892.
- Song, P. X.; Wang, L.; Zhou, Y.; He, J.; Zhu, B.; Wang, F.; Tang, L.; and Eisenberg, M. 2020. An epidemiological forecast model and software assessing interventions on COVID-19 epidemic in China. *medRxiv*.
- Sun, H.; Qiu, Y.; Yan, H.; Huang, Y.; Zhu, Y.; and Chen, S. X. 2020. Tracking and Predicting COVID-19 Epidemic in China Mainland. *medRxiv*.
- Tildesley, M. J.; Savill, N. J.; Shaw, D. J.; Deardon, R.; Brooks, S. P.; Woolhouse, M. E.; Grenfell, B. T.; and Keeling, M. J. 2006. Optimal reactive vaccination strategies for a foot-and-mouth outbreak in the UK. *Nature* 440(7080): 83–86.
- van Hasselt, H. P.; Hessel, M.; and Aslanides, J. 2019. When to use parametric models in reinforcement learning? In *Advances in Neural Information Processing Systems*, 14322–14333.
- Van Moffaert, K.; Drugan, M. M.; and Nowé, A. 2013. Scalarized multi-objective reinforcement learning: Novel design techniques. In *2013 IEEE Symposium on Adaptive Dynamic Programming and Reinforcement Learning (ADPRL)*, 191–199. IEEE.
- Walsh, T. J.; Nouri, A.; Li, L.; and Littman, M. L. 2009. Learning and planning in environments with delayed feedback. *Autonomous Agents and Multi-Agent Systems* 18(1): 83.
- Wilson, S. 2020. Pandemic leadership: Lessons from New Zealand’s approach to COVID-19. *Leadership* 1742715020929151.
- Zhang, J.; Lou, J.; Ma, Z.; and Wu, J. 2005. A compartmental model for the analysis of SARS transmission patterns and outbreak control measures in China. *Applied Mathematics and Computation* 162(2): 909–924.
- Zlojutro, A.; Rey, D.; and Gardner, L. 2019. A decision-support framework to optimize border control for global outbreak mitigation. *Scientific reports* 9(1): 1–14.